Diffusion of Semi-Flexible Polyelectrolyte Through Nanochannels

Hongyan Gu, Santiago Faucher, and Shiping Zhu
Dept. of Chemical Engineering, McMaster University, 1280 Main Street West, Hamilton, ON, Canada L8S 4L7

DOI 10.1002/aic.12106
Published online November 2, 2009 in Wiley InterScience (www.interscience.wiley.com).

The diffusion of sodium polystyrene sulfonate through polycarbonate nanochanels was studied in salt-free dilute aqueous solution. A stronger molecular weight dependence of diffusion was observed compared to free diffusion in dilute solution. Scaling exponentials relating polymer size to diffusivity were between Flory's theory ($D_{eff} \propto N^{-0.6}$) and Rouse's model ($D_{eff} \propto N^{-1}$), revealing a crossover regime from 3-D diffusion to 1-D diffusion. Diffusion was less hindered for the polyelectrolyte (D_{eff}/D_0), than for a rigid sphere, when the polymer/channel size ratio exceeded 0.2. This is attributed to elongated chains with reduced frictional hindrance. Simulation of the confined diffusion based on an elongated cigar model gave $D \propto N^{-1}R_t^{2/3}$ while the experimental results agree with $D \propto N^{-0.94}R_t^{2/3}$. For charged polyelectrolytes, the transition to 1-D diffusion therefore begins before the polymer radius of gyration exceeds the channel size contrary to model assumptions. We attribute this to the charged nature of the polyelectrolytes causing extended chain conformations. © 2009 American Institute of Chemical Engineers *AIChE J,* 56: 1684–1692, 2010
Keywords: diffusion, nanochannel, polyelectrolyte, semi-flexible chain, membrane

Introduction

Polymer diffusion in a confined geometry has been an appealing topic for both experimental and theoretical studies given its practical importance in the fields of molecular separation, catalysis, and bio-electrophoresis.[1–10] In the last few decades, hindered diffusion of colloids or flexible polymers in synthetic membranes has been studied.[11,12] These studies attempted to analyze hindrance in terms of effective partition of polymers as well as increased drag coefficient inside channels. In these works, most solutes are modeled as either rigid spheres or Gaussian chains and sometimes as porous spheres to derive numerical expressions modeling the diffusion behavior.[13] These models have proven true for the diffusion of spherical solutes, some flexible, and linear polymers as well as branched polymers. However, these theories have seldom been applied to describe and model the diffusion of charged polyectrolytes. In the few cases where polyelectrolyte diffusion has been studied, the mediums used are typically salted causing shielding of electrostatic charges on the chain backbone and therefore diffusion behavior that is artificially akin to that of flexible polymer chains. Although complex, no experimental studies have examined the confined diffusion of highly charged polyelectrolytes with scaling theory and compared the theoretical models in a crossover region from 3-D to 1-D diffusion.

Unlike neutral polymers, polyelectrolytes dissociate in aqueous solution to form polyions and numerous counterions. In the presence of adequate electrolyte salt (e.g., NaCl), the counterions screen the charges of the polyion. However, with low or zero-salt concentration, the polyions are known to behave as wormlike (or semi-flexible) chains because of the electrostatic repulsion between charges along the chains.[14–17] Therefore, charged polyelectrolyte chains are more extended than neutral flexible polymer chains. Usually, a wormlike chain is characterized by its contour length L, being the length along the chain contour and the persistence length l_p, a length scale for measuring polymer bending rigidity. The concept of persistence length was first introduced by Kratky and Porod, as a direct measure of local conformation for a linear polymer chain in small-angle scattering experiments.[18,19] Later, it was further developed in

Correspondence concerning this article should be addressed to S. Zhu at zhuship@mcmaster.ca

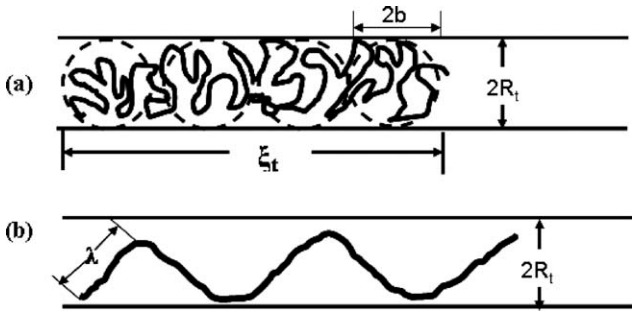

Figure 1. Conformation of a single polymer chain trapped into a cylindrical tube with tube diameter = $2R_t$.

(a) Blob model: an elongated polymer chain inside a small tube is simulated as a series of blobs where b is the radius of blob, ξ_t is the axial extension of polymer chain inside the tube. (b) Odijk model: a highly confined polymer chain inside a small tube is schemed as a more extended chain with a characteristic reflecting length of λ.

relation to ionic strength to describe bending rigidity of semi-flexible polyelectrolyte. A longer persistence length is indicative of a relatively stiffer chain.

The static size of polyelectrolyte chain is directly related to its persistence length. In a bulk solution, where no confinement is present, a wormlike swollen chain has a radius of $R_f \approx N^{3/5}\, a\, (l_p/a)^{1/5}$ according to Flory's theory,[5] where a is the size of monomeric unit and N is the degree of polymerization. Its free diffusivity thus scales as: $D_0 \propto N^{-3/5}\, a^{-1}\, (a/l_p)^{-1/5}$ once one incorporates the prior equation into the Einstein equation ($D_0 \propto k_BT/R_f$) relating the rate of diffusion of a rigid sphere to its size. Given a fixed persistence length, this model therefore predicts that the diffusivity of polymer chain is inversely proportional to its chain length (N, or alternatively molecular weight) to the power of 0.6.

In narrow channels, the chains are also free to coil so long as the channel radius R_t is larger than the coil size. However, if the coil size exceeds channel size, the polymer chain must elongate to pass through the channel. de Gennes and coworkers.[1,5] presented an elongated cigar model for the diffusion of polyelectrolyte chains in a cylindrical tube when the tube diameter is larger than the polymer persistence length ($2R_t > l_p$). The polymer chain is viewed as a connected sequence of blobs having a radius of b (Figure 1a, $b = R_t$). The diffusion coefficient of the blob chain (or elongated cigar) inside tube is estimated to be: $D_{blob} \propto (aN)^{-1}(R_t/a)^{2/3}(a/l_p)^{1/3}$. For constant a and l_p, the diffusivity D_{blob} is proportional to $N^{-1}R_t^{2/3}$. The blob model is based on the assumption that the tube is filled with an extended polymer when the tube size is equal to the blob size. de Gennes' model therefore predicts that the diffusivity is inversely proportional to the number of repeat units in the polymer chain (or alternatively molecular weight).

For stronger confinements where the persistence length is larger than the tube size ($2R_t < l_p$), back-folding of a polymer chain is energetically unfavorable. The chain then presents a "reflecting" conformation.[20] In this case, a length scale of $\lambda \approx (2R_t)^{2/3}\, l_p^{1/3}$ was introduced by Odijk to study chain dynamics. Below this length scale, the chain segment is treated as rigid rod and the whole chain can be considered as a sequence of rigid links (Figure 1b). On the basis of the Odijk model, the diffusivity was derived as: $D_{Odijk} \propto N^{-1} \ln(R_f/w)$, where w is the width of the rod.[21–23] Both Odijk's and de Gennes' models for confined systems therefore estimate the diffusivity to scale with the inverse of polymer molecular weight. These models therefore are in sharp contrast to those modeling diffusion behavior in a bulk system where the diffusivity is proportional to $N^{-0.6}$.

The Odijk and de Gennes models describe isolated, elongated polymer chain dynamics in a tube. Although these scenarios are interesting theoretically, they are difficult to verify experimentally. However, in cases where polymer chains are moderately confined and in a crossover regime between bulk and confined diffusion, experimental validation of these models may be possible. In this work, we experimentally investigate the diffusion of charged sodium polystyrene sulfonate (PSS) chains through cylindrical nanochannels in dilute salt-free solution for the first time. The effects of polyelectrolyte chain length and channel size on the diffusion are examined and compared with different theoretical models. The radii of the nano-channels used in this study are comparable or larger than the hydrodynamic radii of the PSS coils with no more than one order of magnitude in difference. Although theoretical models rely on channel size to define a deforming limit which is difficult to realize in experiments, the study of crossover behavior in confined spaces is experimentally feasible. This work provides new experimental evidence for the early transition between 3-D and 1-D diffusion for highly charged polyelectrolyte not previously explored.

Experimental

Materials

Sodium polystyrene sulfonate (PSS) standards prepared by sulfonation of polystyrene standards were purchased from Polymer Standards Service-USA Inc. The degree of sulfonation ranges from 85% to 90% as reported by the manufacturer. The weight average molecular weights of these polymers are listed in Table 1. The polydispersivity indexes (M_w/M_n) of the parent polystyrene standards are lower than 1.04. Sodium benzoate (Fluka, 99.5%) was used as received. Solutions were prepared with filtered de-ionized Water from

Table 1. Characteristics of PSS Standards and Channel Properties of Polycarbonate Membranes in this Study

			R_H/R_t		
M_W (kg/mol)	R_H* (nm)	R_g † (nm)	R_t‡ = 16 nm P§ = 0.96%	R_t = 27 nm P = 1.32%	R_t = 40 nm P = 4.1%
6.53	1.9	2.9	0.12	0.07	0.05
15.0	3.1	4.9	0.19	0.11	0.08
32.9	5.1	7.9	0.32	0.19	0.13
63.9	7.6	11.8	0.48	0.28	0.19
145	12.4	19.5	0.78	0.46	0.31

*Hydrodynamic radius of polyelectrolyte was calculated based on Stokes-Einstein equation: $R_H = k_BT/6\pi\eta D_0$, where k_B is Boltzmann's constant, T is the absolute temperature, η is the viscosity of water and D_0 is the free diffusivity of the solute.[25]

†Radius of gyration was calculated by $R_g \cong 0.0829 k_BT/\eta D_0$.[25]

‡Radius of nanochannel was averaged by SEM images.

§Porosities, i.e., the ratio of effective diffusion area over membrane surface area, was measured by small solute diffusion experiments, using the same apparatus shown in Scheme 1.

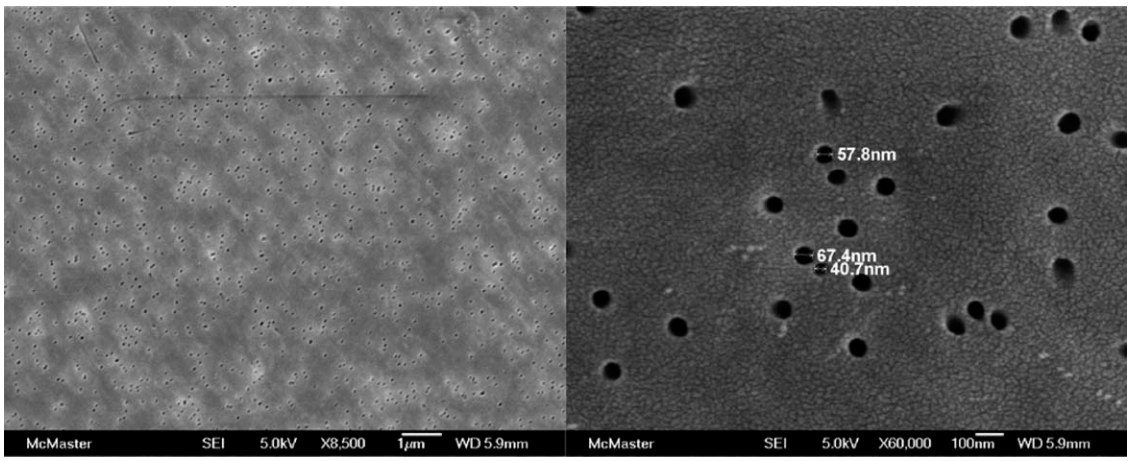

Figure 2. Examples of PC membrane micrographs by SEM (average $R_t \approx 27$ nm).

a Milli-Q water purification unit. Track-etched polycarbonate (PC) membranes with uniform parallel cylindrical pores were sourced from Sterlitech Corp with the membrane sizes also listed in Table 1.

Membrane characterization

SEM Scanning electron microscopy (JEOL JSM-7000F SEM) was used to characterize the pore sizes and uniformity of the nanochannels. Track-etched PC membranes were coated with gold by vacuum deposition before imaging. Two representative SEM photographs of the track-etched PC membrane are shown in Figure 2. From the images, it is evident that the pore size distribution and pore density are uniform. The pores are aligned normal to the membrane surface, so that the pore length (l) is considered to be equivalent to the membranethickness.

Small Solute Diffusion Experiments. The diffusion of sodium benzoate through the PC membranes was measured using the diffusion apparatus, shown in Scheme 1, to determine porosity of the membranes before their use for the study of polymeric diffusion. As the molecular size of sodium benzoate is much smaller than the membrane pore size ($R_H/R_t < 0.01$), hydrodynamic hindrance from the membrane can be neglected. The free diffusion coefficient of sodium benzoate is $D_{\text{benzoate}} = 8.63 \times 10^{-6}$ cm^2/s as reported in the literature.[24] Taking this value as the effective diffusion coefficient, the membrane porosity can be calculated using mass transfer equation (Eq. 1). The porosity results of three different membrane samples are listed in Table 1.

Diffusion experiments

The diffusion experiments were conducted in a custom fabricated diffusion cell at room temperature (23°C). The cell was made by incorporation of a custom fabricated Teflon cap to a UV quartz cuvette (Scheme 1). The cap was designed to seal the cuvette and simultaneously fix the track-etched PC membrane to its top. In so doing, the quartz cuvette became the donor chamber while the Teflon cap served as part of the receiving chamber side of the diffusion apparatus. In this way, the solute concentration in the donor chamber could be measured on-line without invasive sampling using a UV spectrophotometer. The donor chamber was stirred by magnetic stirring and the receptor side refreshed through a re-circulating water circuit pumping fluid at a rate of 0.8 ml/min. The experimental time depended greatly on the ratio of polymer size to pore size and ranged from 5 h to 60 h as this ratio increased. Each experiment was repeated three to four times to obtain an average diffusivity.

Estimate of diffusion coefficient

For membrane transport at pseudo-steady state, a mass balance equation across the membrane is given by:

$$\frac{dn}{dt} = kA(c_2 - c_1) \tag{1}$$

where dn/dt is the flux of solute transfer in moles/s, k is the total mass transfer coefficient, and A is the membrane area. With the initial conditions of $c_1 = 0$ and $c_2 = c_{2,0}$ at $t = 0$ and approximating $c_1 \approx 0$ during the length of the experiment ($V_1 \gg V_2$), integrating Eq. 1 yields:

$$\ln\frac{\Delta c_t}{\Delta c_0} = -\frac{kA}{V_2}t \tag{2}$$

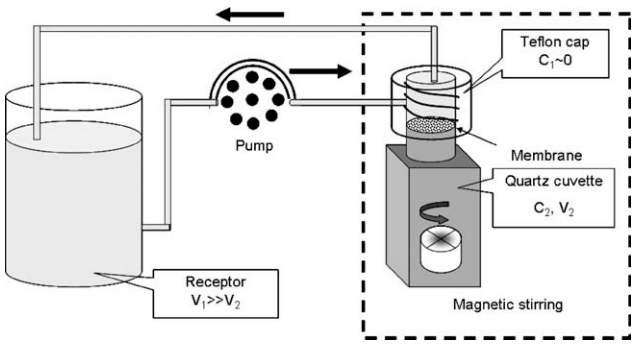

Scheme 1. The on-line diffusion cell setup based on a UV-spectrometer method.

c_1, c_2 denotes the solute concentration in the receptor and donor chamber, and V_1, V_2 are the volumes of receptor and donor chamber. Apparatus are not to scale.

Table 2. Summary of PSS Diffusion Coefficient Data in PCTE Membranes

M_W kg/mol	$D_0 \times 10^{-7}$ cm^2/s	$R_t = 16$ nm		$R_t = 27$ nm		$R_t = 40$ nm	
		$D_{eff} \times 10^{-7}$cm^2/s	D_{eff}/D_0	$D_{eff} \times 10^{-7}$cm^2/s	D_{eff}/D_0	$D_{eff} \times 10^{-7}$cm^2/s	D_{eff}/D_0
6.53	12.9	6.81	0.53	9.23	0.725	11.56	0.89
15.0	7.84	3.55	0.45	4.99	0.64	6.127	0.78
32.9	4.84	1.52	0.31	2.56	0.53	3.35	0.69
63.9	3.23	0.81	0.25	1.45	0.45	2.12	0.66
145	1.96	0.29	0.15	0.45	0.24	0.75	0.38

where V_2 is the volume of donor chamber, t is the duration of measurement (typically between 5 and 60 h), and Δc_t and Δc_o are the solute concentration difference between two chambers at time t and the beginning, respectively. The inverse of mass transfer coefficient ($1/k$) is the mass transfer resistance, which is composed of the membrane resistance (l/pD_{eff}), the entrance/exit effects ($\pi R_t/4pD_0$) and the boundary layer resistance (δ/D_0) on both sides of the membrane. The following approximation was derived by Malone and Anderson[26]:

$$\frac{1}{k} = \frac{l}{D_{eff}p} + \frac{\pi R_t/2}{D_0 p} + \frac{2\delta}{D_0} \tag{3}$$

where D_{eff} is the effective diffusion coefficient inside pores, p is membrane porosity, and δ is the boundary layer thickness on each side of the membrane. The entrance/exit effect adds two equivalent transfer length of $\pi R_t/4$ to the total path in pores. As the channel length used here is 6 μm, and the pore radii range from 16 to 40 nm, the maximum end effect to membrane transport is less than 1%. Considering the effective diffusion coefficients of PSS in membranes were much smaller than that in bulk, the end effect to membrane transfer resistance is negligible.

On the other hand, the boundary layer thickness δ is correlated with bulk diffusivity at a fixed stirring rate based on Colton and Smith's prediction[27]:

$$\delta \propto D_0^{1/3} \tag{4}$$

Thus Eqs. 3 and 4 implies the boundary layer resistance becomes more significant for small, fast diffusing solutes transport through membrane.[9] In the worst case when the smallest PSS ($M_W = 6530$ g/mol) diffuse through the largest pores ($R_t = 40$ nm), the maximum boundary layer effect was about 20% of the total resistance. Our results were also compared with literature measurement on the same type of track-etch membrane with similar pore sizes.[28,29] The membrane boundary layer effect can also be estimated by analytical method,[30] given that the membrane used here has very low porosity and the diffusion experiments were conducted under sufficient stirring.

Results and Discussion

Table 2 summarizes our experimental results. The diffusion coefficient of sodium polystyrene sulfonate inside the track-etched polycarbonate membrane nanochannels clearly decreased with increasing polymer molecular weight, M_W, and increased with increasing nanochannel radius, R_t. The polymer's free diffusion coefficient in the diluted bulk solution, D_0, was obtained through extrapolation of the diffusion data of highly charged PSS to infinite dilution by Tanahatoe and Kuil.[31] The effective diffusion coefficient of the polyelectrolyte through the nanochannel, D_{eff}, was measured by the UV diffusion cell in a dilute solution with the polyelectrolyte concentration less than 1/10 of the overlap concentration of each polymer, typically in the range of $c_2 = 0.5$–1.0 g/l.

Dependence of diffusion coefficient on polymer molecular weight

The diffusion coefficient is predicted to be proportional to $N^{-0.6}$ for a molecule following a self-avoiding random walk in a good solvent (N is the number of repeat units in the polymer chain, and N is proportional to M_W). It is known that direct measurement of the charged polyelectrolyte diffusion at infinitely low concentrations and in salt free solution is not feasible, as there are some extraordinary phenomena still controversial. Tanahatoe and Kuil[31] analyzed their diffusion data in a salt system and showed the molar mass dependence of diffusion $D_0 \propto N^{-0.61}$, which is in agreement with polymer self-avoiding walk theory. However, in our work, the presence of nanochannels caused a stronger dependence of diffusion on molecular weight. As observed in Figure 3, the slope of the best linear fit provides a power

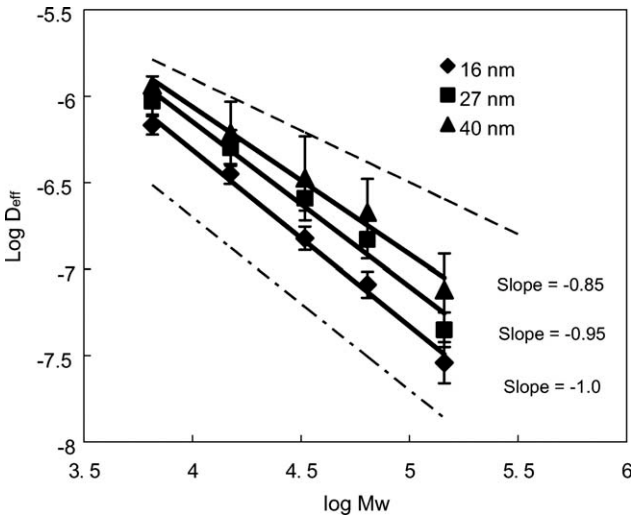

Figure 3. Effective diffusivity as a function of molecular weight (M_W) for varying nanochannel sizes in a logarithm scale.

The dashed line (slope of -0.6) and dash-dot line (slope of -1.0) represent the expected slope for free diffusion (3-D, Flory) of polymer chains in a good solvent and for constrained diffusion of polymers in channels (1-D, de Gennes, Rouse, and Pincus) respectively.

law index of the molecular weight dependence for each set of experiments with a fixed pore size. As the nanochannel size decreased from 40 nm to 16 nm, the exponent on molecular weight relating to diffusion decreased from −0.85 to −1, owing to the increased constraints from the channel wall ($D \propto M^{-0.85}$ to M^{-1}). In the smallest channel size ($R_t = 16$ nm), where the polymer/pore size ratio (R_H/R_t) ranged from 0.12 to 0.78, the molecular weight dependence of diffusion was very close to ($D \propto M^{-1}$) intending to show the trend of Rouse behavior. However, the trend doesn't persist for a long range and the last set of data emerges to be a bit offline indicating a larger molecular dependence. The trend we observed for the polyelectrolytes through the precisely perforated polycarbonate membranes is comparable to that for polystyrene diffusion through non-structured porous glass. Guo et al.[32] reported that the diffusion of polystyrene through porous glass was inversely proportional to molecular weight when the polymer/pore size ratio (R_H/R_t) was between 0.2 and 0.5. When $R_H/R_t > 0.6$, a stronger molecular weight dependence ($D \propto M^{-v}$, $v > 1$) was observed. In their work, however, the pore structure in the porous glass was highly inter-connected and tortuous making it difficult to determine the diffusion path length and pore size. To address this, they used a correction method based on "cavity and bottleneck models" to give an average value. In contrast, our approach did not require this correction as the nanochannels were well defined. The nanochannels in the PC membranes were isolated fine cylindrical tubes with high uniformity and therefore the influence of geometrical defects was not expected. Nevertheless, Guo's work provided interesting data describing a behavior akin to that we observed in this work for a fine structure now commercially available.

The data in Figure 3 suggest a transition from 3-D diffusion to 1-D diffusion, taking place in the range of medium confinements ($0.12 < R_H/R_t < 0.78$). It should be pointed out that de Gennes' 1-D elongated cigar model postulated the blob size equal to the tube size and the confined chain aligned in the axis of the tube (Figure 1a). In such a scenario, one would expect that the confined polymer chain has a R_H much larger than the tube size R_t. This appears not to be the case in our work because we observed the linear molecular weight dependence of diffusivity to occur at $R_H/R_t <$ 0.78. Furthermore, experimental data indicates the trend of molecular weight dependence tends to be larger as the extent of constraint (R_H/R_t) increases. Whether this trend is a continuous evolution or sudden transition need to be further investigated. It seems to be beyond the limit of our measurement to expand the constraint range, as the diffusion of larger PSS standards through these membranes is extremely slow. It is not well understood what will happen when the polymer chain size approach the channel size, but the trend is clear that a larger molecular weight dependence (power law index <-1) of the constrained diffusion should occur at $R_H = R_t$.

Pincus modeled the dynamics of an isolated and stretched chain in a good solvent under external force (hydrodynamic fluctuations, velocity gradients, or electrical fields, etc.) instead of the geometrical confinement.[33,34] On the basis of scaling theory, Pincus applied a tensile force f to the end of polymer chain. The stretched chain was represented as a sequence of blobs with the blob size

$$b_{\text{Pincus}} = k_B T/f \tag{5}$$

In contrast to de Gennes' confined chain, the stretched chain allowed for lateral fluctuations within a small range, but this difference did not affect the scaling law of chain dynamics. Therefore, the simulated dynamics of both chains were similar except for their numeric coefficients.[1] That is, if the confined chain in a narrow tube in de Gennes' theory is replaced by Pincus' elongated chain with smaller blob sizes, using the Kirkwood calculation method to determine chain mobility, the diffusion coefficient inside tubes scales analogously as $D \propto N^{-1}$. Both de Gennes and Pincus scalings are based on the assumption that cooperative motion of the segments due to hydrodynamic interaction is negligible, which result in a "free draining" motion style in consistent with the Rouse diffusion model ($D_{\text{Rouse}} = k_B TB/N$ or $D_{\text{Rouse}} \propto N^{-1}$, where B is the monomer mobility in solution).[35] One should note that the scaling of diffusivity with chain length isolates hydrodynamic interactions but the channel size is also a combined effect which is related to the conformation of the chain and the drag on segments. In the following section, the diffusion data is analyzed in a different approach accounting for both polymer size and channel size effect.

Comparison with rigid sphere model

In many engineering situations, the diffusion of polymers in porous membrane or small channels is characterized in terms of diffusion hindrance, which is defined as the ratio of effective diffusion coefficient over free diffusion in solution (D_{eff}/D_0). The diffusion hindrance is considered as a product of partition coefficient and hydrodynamic interaction between chain and wall.[11] In this manner, Renkin modeled the diffusing solute as a rigid sphere that is geometrically constrained by the centre line of a confining cylindrical pore[7]:

$$\frac{D_{\text{eff}}}{D_0} = \left(1 - \frac{R_H}{R_t}\right)^2 \times \left[1 - 2.1\left(\frac{R_H}{R_t}\right) + 2.1\left(\frac{R_H}{R_t}\right)^3 - 0.95\left(\frac{R_H}{R_t}\right)^5\right] \tag{6}$$

The first term in the product represents the reduction of effective diffusion area when the solute has a finite size, as a result of steric exclusion from the pore wall. In other words, the effective diffusion channel is smaller in its cross section than the entire channel, because the center of particle (or centre of mass) can only pass through an area with a radius of ($R_t - R_H$).[36] In an deal case, this term is approximately equal to the partition coefficient of a spherical solute in a cylindrical channel. The partition coefficient is defined as the ratio of polymer concentration inside a porous media over the concentration outside of it when the system reaches an equilibrium.[12] The second term in the product is the friction factor between solute and pore wall, theoretically derived by Faxen.[37,38] This equation was extensively verified by confined diffusion experiments of urea, glucose, antipyrine, sucrose, in porous membranes, typically when $R_H/R_t < 0.32$. In addition, subsequent studies on the diffusion of linear polymers in track-etched membranes or other porous membranes were also reported for testing the theory with the polymer/pore size ratios up to 0.8.[9,10,39–41] A very good review paper by Deen compared the existing theoretical

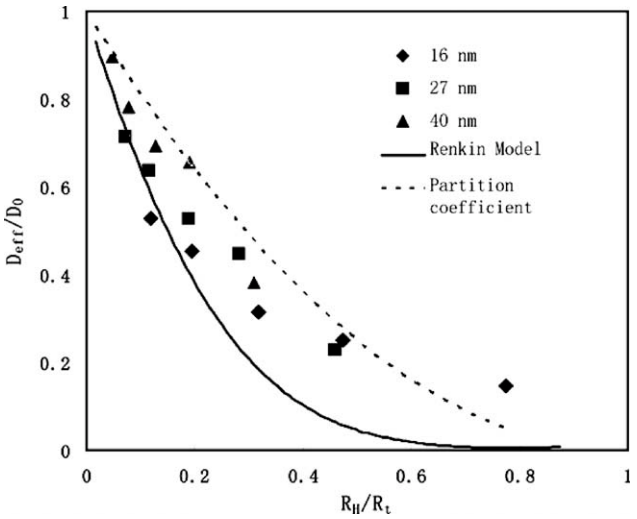

Figure 4. Plot of the effective-to-free diffusivity ratio as a function of polymer-to-pore size ratio.

Solid curve represents Renkin's model. Dashed curve is the reduced partition coefficient of spherical solute inside the cylindrical channel as a function of the polymer/pore size ratio estimated by $(1-R_H/R_t)$.[2]

models with some spherical solute diffusion experiments in membranes having cylindrical pores.[11] In most of these studies, flexible linear polymer chains were adequately large to be treated as hydrodynamic particles or porous rigid spheres, given a characteristic size of R_g or R_H.

Figure 4 shows that D_{eff}/D_0 decreased as the polymer/pore size ratio R_H/R_t increased. This is expected because there was a reduced partition of solute inside the nanochannels as compared to the bulk condition. At higher R_H/R_t ratios, the effective diffusion of PSS was significantly faster than the predicted. If we eliminate the hydrodynamic friction effect in the model (i.e., the second term in the product in Eq. 6), the predicted partition coefficient (the dashed curve in Figure 4) is close to the experimental data. The frictional hindrance from the channel wall on the polymer is therefore noted but its effect is smaller than that predicted by a rigid sphere model.

A similar deviation from the Renkin model was reported by Deen et al.[29] for the hindered diffusion of dextran and ficoll polymer through PC membranes. Dextran is a linear polysaccharide while ficoll is a crosslinked copolymer of sucrose and epichlorohydrin. Both polymers were selected with a series of molecular weights having similar hydrodynamic radius, with the polymer/pore size ratio ranging from 0.2 to 0.8. It was found that within the same PC microchannels, linear dextran diffusion was faster than that predicted by the rigid sphere model while ficoll diffused remarkably slower than the predicted. It was postulated that the deformation of linear chains inside the pores could potentially reduce the frictional hindrance from the wall thus allowing for faster diffusion rates than rigid spherical molecules (ficoll).

The measurement of the size effect on diffusion inherently depends on the method used for measuring polymer configuration (R_H). Our calculation of PSS molecule size was based on the Stokes-Einstein equation, which is the equivalent hydrodynamic radius of a spherical solute having the same diffusion coefficient. This definition is extensively used for coiled polymer diffusion in unbounded solutions. However, it is not a true radius defining the boundary of a polymer chain. Particularly, for polymer chains possessing irregular or elongated configuration, the radius dimension is just a characteristic length scale related to its mobility. To gain perspective on the rigidity of polyelectrolytes in regards to diffusion hindrance, we examined the literature data related to persistence length, Debye screen length, and contour length scale.[17,21,22,31] The PSS chain length information is summarized in Table 3 and analyzed later.

The stiffness of a charged polyelectrolyte chain can be characterized by its contour length L and persistence length l_p. On the basis of the study of Kassapidou et al.[42] the persistence length l_p for PSS in a salt-free solution is 15.8 nm and 18.6 nm at ionic strengths of 0.004 and 0.001 mol/L. Lower ionic strength results in longer l_p for the same polyelectrolyte since the charges on the backbone are not as effectively screened. An estimate of the confined PSS l_p in this work is difficult because the polyelectrolyte concentration and counterions are restricted by the channel size. If we assume the concentration of monomer units inside the channel is governed by the partition effect only and the counterions distribute homogeneously in the system, the monomer concentration inside the channel can be estimated as:

$$c_{m,tube} = (1 - R_H/R_t)^2 c_{m,bulk} \tag{7}$$

where $c_{m,tube}$ is always lower than 0.004 mol/L. The PSS persistence lengths in this study are therefore $l_p > 15.8$ nm. This length scale is most likely in the same order of magnitude with the contour lengths L of the five PSS standards listed in Table 3. Therefore, we can consider the polymer chains to be extended and rod like in their conformation.

A second challenge in determining charged chain conformation relates to the electrostatic interactions that occur in salt-free solution, which is usually modelled with the Debye-Huckel approximation.[23] On the basis of the assumption that there is no inter-chain charge stiffening, and electrostatic

Table 3. Molecular Weight (M_W), Number of Repeat Units (N), and Contour Length (L) of the Sodium Polystyrene Sulfonate (PSS) Standards Without Added Salt in Dilute Solution

PSS standards	Standard 1	Standard 2	Standard 3	Standard 4	Standard 5
M_W (kg/mol)	6.53	15.0	32.9	63.9	145
N*	32	73	160	310	704
$L^\dagger$ (nm)	5.4	12.4	27.2	52.7	120

*Degree of polymerization, derived from polymer molecular weight (M_W) divided by monomer molecular weight.
†Contour length calculated with the monomeric distance = 0.17 nm.[31]

screening is only caused by noncondensed counterions, the calculation of Debye-Huckel screening length (κ^{-1}) for salt-free polyelectrolytes can be simplified to[23,43]

$$\kappa^{-1} = (4\pi l_B c_m)^{-1/2} \tag{8}$$

where l_B is the Bjerrum length, c_m is the monomer concentration in a unit volume. This equation shows the Debye-Huckel screen length is directly determined by the monomer concentration, lower concentration results in longer screen length with square-root dependence. Given a Bjerrum length of 0.7 nm for water at 25°C, and an average monomer concentration of 0.002 mol/l in this study, κ^{-1} is estimated to be 7.8 nm. This screen length is in the order of the persistence length scale, and is comparable to R_g of most of the polyelectrolyte standards. Again this indicates polymer chains are significantly stiffened by the electrostatic interaction between monomers, and likely take on an elongated configuration.

Park et al. studied the statistical mechanics of polyelectrolyte in cylindrical pores with a Gaussian chain assumption based on a Debye-Huckel screen length.[44,45] Taken into account were the effects of screened electrostatic interactions and the excluded volume effect between monomeric unit and pore wall as well as between monomeric unit pairs. Neglecting the counterion condensation, they found a crossover of chain conformation from stretched ($R_g \propto L$ if $R_g \leq \kappa^{-1}$) to self-avoiding chain ($R_g \propto L^{3/5}$ if $R_g > \kappa^{-1}$) regime. If we apply Park's simulation to the present work, the PSS standards 1 to 4 would have a stretched conformation as R_g is in the same magnitude of κ^{-1}. However, the equilibrium partition concentration of Sample 5 with a large coil size is significantly reduced as the polymer size approaches the channel size. That is, the electrostatic screening length scale would increase according to Eq. 8. Again, although the R_g of Sample 5 in bulk is about 19.5 nm, which appears sufficiently long to behave as a self-avoiding coil, when confined in the channels with $R_t = 16$, 27, 40 nm, the partition concentration of the large PSS inside channels would be reduced to a factor of 0.05, 0.29, or 0.48 of the bulk concentration, respectively. This dilution thus leads to longer Debye-Huckel screening lengths of up to 30 nm in small channels. Therefore, the large polyelectrolyte chain would also deform and elongate inside the small channels. This rigid extended chain conformation explains the enhanced molecular weight dependence of diffusion in nanochannels and thus following a different hindrance model in comparison with the solid sphere model.

Scaling of diffusivity based on elongated blob chain model

Given the lack of a complete fit with the rigid sphere model, and the indication of extended conformation for most of the polymer samples inside nanochannels, we correlated our data to the theories pertaining to chains that are stretched such as de Gennes' elongated cigar model or Odijk's theory. The crossover behavior between de Gennes and Odijk regimes is currently not fully understood. However, we can speculate that Odijk's model is better suited than de Gennes' cigar model to account for diffusion of polymers under stronger confinement. A rough critical confinement size was identified by Reisner et al by measuring DNA extension and relaxation time inside square shaped nanochannels (channel width ranged from 30 to 400 nm). They found the crossover behavior between de Gennes and Odijk's regimes when the channel width is about twice of the DNA persistence length.[46] Below this critical width, bending rigidity becomes significant (Odijk's model) and power law scaling of relaxation time with channel width disagrees with de Gennes' prediction. If we equate the cylindrical channel diameter with square channel width in this study, the three membrane diameters ($2R_t = 32$, 54, 80 nm) are generally over twice of the polyelectrolyte persistence length (15–18 nm). That is, the polyelectrolyte chains should retain bending and back-folding segments, which could be better explained by the blob model.

Given that the hydrodynamic radii or radii of gyration of the present polymer standards are smaller than the radii of channels in the membranes, the lateral dimension of stretched chains should have even smaller size if they orient along the nanochannel axis. To apply the blob chain model in this study, we hence assume the equivalent blob size (b) of a confined polyelectrolyte chain is $b = \gamma R_t$, where γ is a constant factor less than 1. Therefore the number of monomeric units inside a blob is defined as:

$$g = (\gamma R_t/a)^{1/v} \tag{9}$$

where v is Flory exponent = 3/5, a is the monomer size. The dimension of the polymer chain inside channel ($l_{||}$) therefore is:

$$l_{ll} = N^*(\gamma R_t) = (N/g)(\gamma R_t) = (aN)(\gamma R_t/a)^{-2/3} \tag{10}$$

where N^* is the number of blobs ($N^* = N/g$). The friction coefficient of the polymer chains inside the channel is thus

$$\zeta_{chain} = 6\pi\eta l_{ll} \tag{11}$$

Finally, the diffusion coefficient inside the channel is described by:

$$D_{eff} \propto \frac{T}{6\pi\eta l_{ll}} \propto (aN)^{-1}\left(\frac{\gamma R_t}{a}\right)^{2/3} \tag{12}$$

Given that a and γ are numerical constants, a simplified scaling law of diffusion as a function of chain length and channel size is:

$$D_{eff} \propto N^{-1}R_t^{2/3} \tag{13}$$

To test the applicability of Eq. 13, the effective diffusion coefficient of the five standards over the channel sizes to the power predicted by the blob theory was plotted against molecular weight. As shown in Figure 5, the majority of the data points fall nicely onto a master curve with a slope = −0.94, which is close to the −1 power predicted for elongated chain diffusion. One might expect diffusion of polyelectrolytes in salt-free solution thus can be modelled as extended molecules moving in a free draining style with screened hydrodynamic interaction. However, the consistency of our diffusion data with blob model is intriguing.

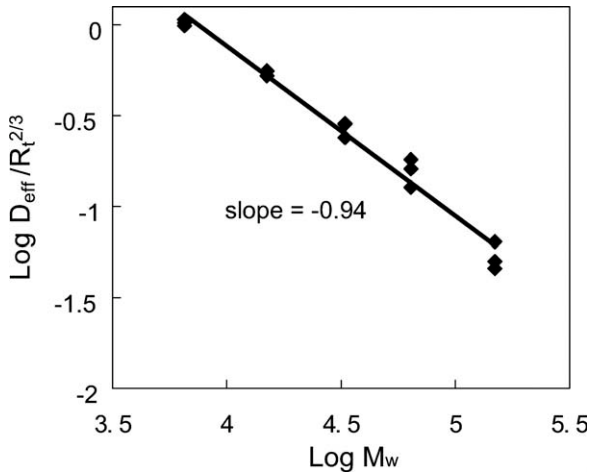

Figure 5. Effective diffusivity divided by the channel radius to the 2/3 power versus PSS molecular weight.

Again it should be pointed out that de Gennes' blob model postulates a long chain molecule "squeezed" inside a very narrow tube where the R_g of polymer chains are much larger than the tube radius. Nevertheless, this appears not to be the case in our work, as the polymer chains are generally smaller than tube sizes. In addition, we realized that most of the polyelectrolyte chains studied here might not be long enough for the "long chain assumption" when deriving those scaling equations. Other effects, e.g., electrostatic potential (Debye screening length) and energy depletion regarding to polymer/wall interaction could be further investigated. We here provide some evidence for a crude analysis and leave the questions open for future discussion.

Conclusion

We studied the confined diffusion of polyelectrolyte in a salt-free environment through PC membrane nanochannels with the polymer/pore size ratios ranged from 0.05 to 0.78. Scaling of the effective diffusion coefficient versus molecular weight revealed a diffusion mechanism that is distinct from that observed in bulk (i.e., self-avoiding walk) with $D_0 \propto N^{-3/5}$. The chain length dependence of the effective diffusion inside the nanochannels ranged from $D_{\text{eff}} \propto N^{-0.85}$ to $D_{\text{eff}} \propto N^{-1}$ as the channel size decreased. Although the equivalent hydrodynamic radii of polymers were smaller than the nanochannel sizes, the inverse proportion of diffusion coefficient with chain length was indicative of 1-D diffusion behavior. The hindrance of confined diffusion coefficient of such polyelectrolyte was found to be smaller than that of rigid sphere solutes. Scaling of the diffusivity with molecular weight and channel size is fairly consistent with the blob model, which is indicative of elongated/stretched conformation of the polyelectrolyte. The polyelectrolyte chain was viewed as a sequence of blobs with the blob size smaller than the channel size. In agreement with the blob model where the diffusivity was inversely proportional to the degree of polymerization, the experimental data showed a diffusivity proportional to the -0.94 power ($D \sim N^{-0.94} R_t^{2/3}$). This exponent close to unity was interpreted as elongated chain dynamics inside the nanochannel, and further intra-molecular hydrodynamic screening. In conclusion, for the charged PSS in this study, the crossover regime of free diffusion and ideal 1-D diffusion started before the polymer radius of gyration exceeded the channel size, which differs from the typical theoretical assumptions.

Acknowledgments

The authors would like to thank Dr. Carlos Filipe for providing generous access to the UV-spectrometer central to this study. This work was financially supported by NSERC Discovery and CFI/CRC.

Notation

a = size of monomeric unit in semi-flexible chain
A = PC membrane surface area in a diffusion cell
c = polymer concentration in diffusion cell
c_m = monomer concentration in solution for calculation of Debye screen length
Δc = concentration difference across diffusion membrane
D_0 = diffusion coefficient in bulk
D_{blob} = predicted diffusion coefficient based on blob theory
D_{eff} = effective diffusion coefficient as measured
D_{Rouse} = diffusion coefficient in Rouse model
g = number of monomeric units inside a blob
k = mass transfer coefficient
k_B = Boltzmann constant
l = membrane thickness or nanochannel length
l_p = persistence length
l_B = Bjerrum length
$l_{||}$ = dimension of polymer chain inside nanotube based on blob theory
L = length of polymer along its contour
M_W = molecular weight of polymer
n = moles of polymer molecules diffused through porous membrane in diffusion experiment
N = degree of polymerization
N^* = number of blobs in a polymer chain
p = porosity of the membrane (%)
R_g = radius of gyration
R_H = hydrodynamic radius of a polymer chain in solution
R_t = radius of a nanochannel
t = duration of diffusion experiments (s)
T = absolute temperature

Greek letters

δ = boundary layer thickness
γ = the ratio of blob radius over tube radius when a polymer chain was confined in a tube
η = liquid viscosity
κ^{-1} = Debye electrostatic screen length
λ = Odijk length scale
w = width of rod in Odijk model
ζ_{chain} = friction coefficient of a confined chain in a small tube

Literature Cited

1. Brochard F, deGennes PG. Dynamics of confined polymer-chains. *J Chem Phys*. 1977;67:52–56.
2. Kremer K, Binder K. Dynamics of polymer-chains confined into tubes—scaling theory and Monte-Carlo simulations. *J Chem Phys*. 1984;81:6381–6394.
3. Sheng YJ, Wang MC. Statics and dynamics of a single polymer chain confined in a tube. *J Chem Phys*. 2001;114:4724–4729.
4. Wei CY, Srivastava D. Theory of transport of long polymer molecules through carbon nanotube channels. *Phys Rev Lett*. 2003;91:235901-1–235901-4.
5. Brochard-Wyart F, Tanaka T, Borghi N, de Gennes PG. Semiflexible polymers confined in soft tubes. *Langmuir* 2005;21:4144–4148.

6. Yang H, Liu Y, Zhang H, Li ZS. Diffusion of single alkane molecule in carbon nanotube studied by molecular dynamics simulation. *Polymer* 2006;47:7607–7610.
7. Renkin EM. Filtration, diffusion, and molecular sieving through porous cellulose membranes. *J Gen Physiol*. 1954;38:225–243.
8. Kimmich R, Fatkullin N, Mattea C, Fischer E. Polymer chain dynamics under nanoscopic confinements. *Magn Reson Imaging*. 2005;23:191–196.
9. Cannell DS, Rondelez F. Diffusion of polystyrenes through microporous membranes. *Macromolecules*. 1980;13:1599–1602.
10. Davidson MG, Deen WM. Hindered diffusion of water-soluble macromolecules in membranes. *Macromolecules*. 1988;21:3474–3481.
11. Deen WM. Hindered transport of large molecules in liquid-filled pores. *AIChE J*. 1987;33:1409–1425.
12. Teraoka I. Polymer solutions in confining geometries. *Prog Polym Sci*. 1996;21:89–149.
13. Davison MG, Deen WM. Hydrodynamic theory for the hindered transport of flexible macromolecules in porous membranes *J Memb Sci*. 1988;35:167–192.
14. Koene RS, Mandel M. Quasi-elastic light-scattering by poly-electrolyte solutions without added salt. *Macromolecules*. 1983;16:973–978.
15. Sedlak M, Amis EJ. Concentration and molecular-weight regime diagram of salt-free polyelectrolyte solutions as studied by light-scattering. *J Chem Phys*. 1992;96:826–834.
16. Sedlak M, Amis EJ. Dynamics of moderately concentrated salt-free polyelectrolyte solutions—molecular-weight dependence. *J Chem Phys*. 1992;96:817–825.
17. Tanahatoe JJ, Kuil ME. Dynamic light scattering of a flexible highly charged polyelectrolyte in the dilute concentration regime. *Macromolecules*. 1997;30:6102–6106.
18. Porod G. Zusammenhang zwischen mittlerem Endpunktsabstand und Kettenlänge bei Fadenmolekülen *Monats Chem*. 1949;80:251–255.
19. Kratky O, Porod G. Rontgenuntersuchung geloster fagenmolekule. *Rec Trav Chim Pays-Bas*. 1949;68:1106–1122.
20. Odijk T, Houwaert AC. Theory of excluded-volume; effect of a polyelectrolyte in a 1–1 electrolyte solution. *J Polym Sci Part B: Polym Phys*. 1978;16:627–639.
21. Odijk T. Possible scaling relations for semidilute polyelectrolyte solutions. *Macromolecules*. 1979;12:688–693.
22. Odijk T. On the statistics and dynamics of confined or entangled stiff polymers. *Macromolecules*. 1983;16:1340–1344.
23. Balducci A, Mao P, Han J, Doyle PS. Double stranded DNA diffusion in slitlike nanochannels. *Macromolecules*. 2006;39:6273–6281.
24. Landolt H, Bornstein R. *Numerical Data and Functional Relationships in Science and Technology*, 6th ed. Heidelberg: Springer-Verlag, 1969, Vol. II/5a.
25. Teraoka I. *Polymer Solutions: An Introduction to Physical Properties*. New York: Wiley, 2002:239.
26. Malone DM, Anderson JL. Diffusional boundary-layer resistance for membranes with low porosity. *AIChE J*. 1977;23:177–184.
27. Colton CK, Smith KA. Mass transfer to a rotating fluid. II. Transport from the base of an agitated cylindrical tank. *AIChE J*. 1972;18:958–967.
28. Bohrer MP. Diffusional boundary layer resistance for membrane transport. *Ind Eng Chem Fundamen*. 1983;22:72–78.
29. Deen WM, Bohrer MP, Epstein NB. Effects of molecular-size and configuration on diffusion in microporous membranes. *AIChE J*. 1981;27:952–959.
30. Beerlage MAM, Peeters JMM, Nolten JAM, Mulder MHV, Strathmann H. Hindered diffusion of flexible polymers through polyimide ultrafiltration membranes. *J Appl Polym Sci*. 2000;75:1180–1193.
31. Tanahatoe JJ, Kuil ME. Molar mass dependence of the apparent diffusion coefficient of flexible highly charged polyelectrolytes in the dilute concentration regime. *J Phys Chem A*. 1997;101:8389–8394.
32. Guo YH, Langley KH, Karasz FE. Hindered diffusion of polystyrene in controlled pore glasses. *Macromolecules* 1990;23:2022–2027.
33. Pincus P. Excluded volume effects and stretched polymer chains. *Macromolecules*. 1976;9:386–388.
34. Pincus P. Dynamics of stretched polymer chains. *Macromolecules*. 1977;10:210–213.
35. Doi M, Edwards SF. *The Theory of Polymer Dynamics*. Oxford, England: Clarendon Press, 1986.
36. Ferry JD. Statistical evaluation of sieve constants in ultrafiltration. *J Gen Physiol*. 1936;20:95–104.
37. Faxen H. Die bewegung einer Starren Kugel längs der Achse eines mit zäher Flüssigkeit gefullten Rohres. *Ark Mat Astron och Fysik*. 1923;17:27.
38. Bacon LR. Measurement of absolute viscosity by the falling sphere method. *J Franklin Inst*. 1936;221:251–273.
39. Kathawalla IA, Anderson JL. Pore-Size Effects on Diffusion of Polystyrene in Dilute-Solution. *Ind Eng Chem Res*. 1988;27:866–871.
40. Guillot G, Leger L, Rondelez F. Diffusion of large flexible polymer-chains through model porous membranes. *Macromolecules*. 1985;18:2531–2537.
41. Ichimura S, Tsuru T, Nakao S, Kimura S. Analysis of linear macromolecule transport through aluminum anodic oxide membranes by pore model. *J Chem Eng Jpn*. 2000;33:141–151.
42. Kassapidou K, Jesse W, Kuil ME, Lapp A, Egelhaaf S, van der Maarel JRC. Structure and charge distribution in DNA and poly(styrene sulfonate) aqeous solutions. *Macromolecules*. 199;30:2671–2684.
43. Dobrynin AV, Colby RH, Rubinstein M. Scaling theory of polyelectrolyte solutions. *Macromolecules*. 1995;28:1859–1871.
44. Park PJ, Sung W. Dynamics of a polymer surmounting a potential barrier: the Kramers problem for polymers. *J Chem Phys*. 1999;111:5259–5266.
45. Park PJ, Chun MS, Kin JJ. Partitioning and conformational behavior of polyelectrolytes confined in a cylindrical pore. *Macromolecules*. 2000;33:8850–8857.
46. Reisner W, Morton KJ, Riehn R, Wang YM, Yu ZN, Rosen M, Sturm JC, Chou SY, Frey E, Austin RH. Statics and dynamics of single DNA molecules confined in nanochannels. *Phys Rev Lett*. 2005;94:196101–1-196101–4.

Manuscript received Apr. 2, 2009, revision received July 21, 2009, and final revision received Oct. 1, 2009.